Science of the Total Environment 855 (2023) 158605

Contents lists available at ScienceDirect

Science of the Total Environment

journal homepage: www.elsevier.com/locate/scitotenv

Tree-ring anatomy of *Pinus cembra* trees opens new avenues for climate reconstructions in the European Alps

Jérôme Lopez-Saez [a,*], Christophe Corona [a,b], Georg von Arx [c,d], Patrick Fonti [c], Lenka Slamova [a,e,f], Markus Stoffel [a,e,f]

[a] Climate Change Impacts and Risks in the Anthropocene (C-CIA), Institute for Environmental Sciences, University of Geneva, 1205 Geneva, Switzerland
[b] Université Clermont-Auvergne, CNRS Geolab UMR 6042, 63057 Clermont-Ferrand, France
[c] Dendrosciences, Swiss Federal Institute for Forest Snow and Landscape Research WSL, 8903 Birmensdorf, Switzerland
[d] Oeschger Centre for Climate Change Research, University of Bern, 3012 Bern, Switzerland
[e] Department of Earth Sciences, University of Geneva, 1205 Geneva, Switzerland
[f] Department F.-A. Forel for Environmental and Aquatic Sciences, University of Geneva, 1205 Geneva, Switzerland

HIGHLIGHTS

- We test the potential of quantitative wood anatomy (QWA) of *P. cembra* for temperature reconstruction.
- Unlike ring width and maximum latewood density, cell wall thickness (CWT) is a very reliable proxy of past temperatures.
- Radial CWT explains 62 % and >80 % of interannual and decadal April–September temperature variability.
- QWA unveils a dormant potential and opens new avenues for a long-lived, widespread and emblematic alpine species.

GRAPHICAL ABSTRACT

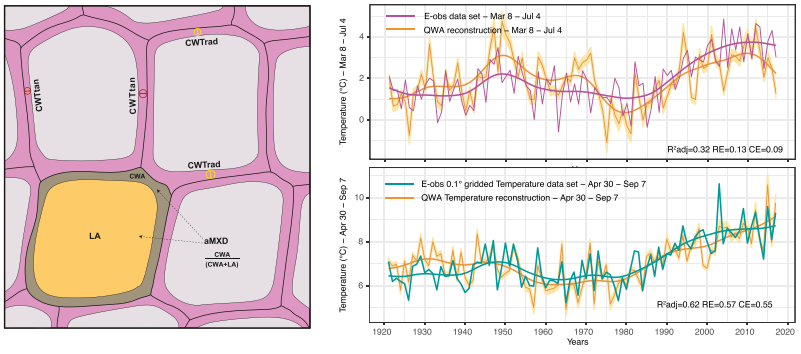

ARTICLE INFO

Editor: Elena Paoletti

Keywords:
Stone pine
Quantitative wood anatomy
Palaeo-climate reconstructions
Growing season temperature
Alps

ABSTRACT

Tree rings form the backbone of high-resolution palaeoclimatology and represent one of the most frequently used proxy to reconstruct climate variability of the Common Era. In the European Alps, reconstructions were often based on tree-ring width (TRW) and maximum latewood density (MXD) series, with a focus on European larch. By contrast, only a very limited number of dendroclimatic studies exists for long-lived, multi-centennial *Pinus cembra*, despite the widespread occurrence of the species at treeline sites across the European Alps. This lack of reconstructions can be ascribed to the difficulties encountered in past studies in extracting a robust climate signal from TRW and MXD chronologies. In this study, we tested various wood anatomical parameters from *P. cembra* as proxies for the reconstruction of past air temperatures. To this end, we measured anatomical cell parameters and TRW of old-growth trees from the God da Tamangur forest stand, known for being the highest pure, and continuous *P. cembra* forest in Europe. We demonstrate that several wood anatomical parameters allow robust reconstruction of past temperature variability at annual to multidecadal timescales. Best results are obtained with maximum latewood radial cell wall thickness (CWTrad) measured at 40 μm radial band width. Over the 1920–2017 period, the CWTrad chronology explains 62 % and >80 % of interannual and decadal variability of air temperatures during a time window corresponding roughly with the growing season. These values exceed those found in past work on *P. cembra* and even exceed the values reported for MXD chronologies built with *L. decidua* and hitherto considered the gold standard for dendroclimatic reconstructions in the European Alps. The wood anatomical analysis of *P. cembra* records therefore unveils a dormant potential and opens new avenues for a species that has been considered unsuitable for climate reconstructions so far.

* Corresponding author.
E-mail address: jerome.lopez-saez@unige.ch (J. Lopez-Saez).

http://dx.doi.org/10.1016/j.scitotenv.2022.158605
Received 8 June 2022; Received in revised form 10 August 2022; Accepted 4 September 2022
Available online 15 September 2022

1. Introduction

Annually resolved and absolutely dated tree-ring chronologies form the backbone of climate reconstructions and represent the most important proxy archive to reconstruct climate variability over past centuries to millennia (Frank et al., 2010; Masson-Delmotte et al., 2013; Büntgen et al., 2009). The tree-ring parameters that were most frequently and successfully used to study temperature variations at high latitudes and altitudes are tree-ring width (TRW) and maximum latewood density (MXD) (e.g., Björklund et al., 2019). In the case of the European Alps, temperature reconstructions are relying mainly on a suite of multi-centennial TRW and MXD chronologies from conifers growing close to timberline (1600–2500 m asl) (Frank and Esper, 2005). Among the available tree species, long-lived and temperature-sensitive European larch (*Larix decidua* Mill.*)* and Swiss stone pine (*Pinus cembra* L.) have the greatest potential for millennium-long reconstructions (see e.g., Corona et al., 2010a, 2010b; Büntgen et al., 2005, 2006). In addition, they often co-occur in the same environment (EUFORGEN, 2014). Yet, whereas L. *decidua* has been used extensively for climate reconstructions (Büntgen et al., 2005, 2006), only very few dendroclimatic studies were based on *P. cembra*, despite the availability of numerous (n = 120) multi-centennial (45 % and 15 % exceed 330 years and 500 years, respectively, Fig. 1A) and high-elevation (80 % of the existing tree-ring records have been sampled above 2000 m asl; Fig. 1B) chronologies.

This imbalance is related to difficulties in extracting a robust signal from *P. cembra* ring width series. Based on a survey of published dendroclimatic studies (Table 1), TRW chronologies of *P. cembra* tend to contain a summer temperature (often June – August, JJA) signal, but with correlations that only rarely exceed r = 0.4 (Carrer and Urbinati, 2004; Leal et al., 2007; Leonelli et al., 2009). They also tend to record a previous-year *(n-1)* – mostly autumn – precipitation or temperature signal (Oberhuber, 2004; Carrer, 2011; Carrer et al., 2007; Oberhuber et al., 2008; Saulnier et al., 2011). The imbalance holds true also for the density signal. The thin latewood - characteristic of the species – has been reported repeatedly to

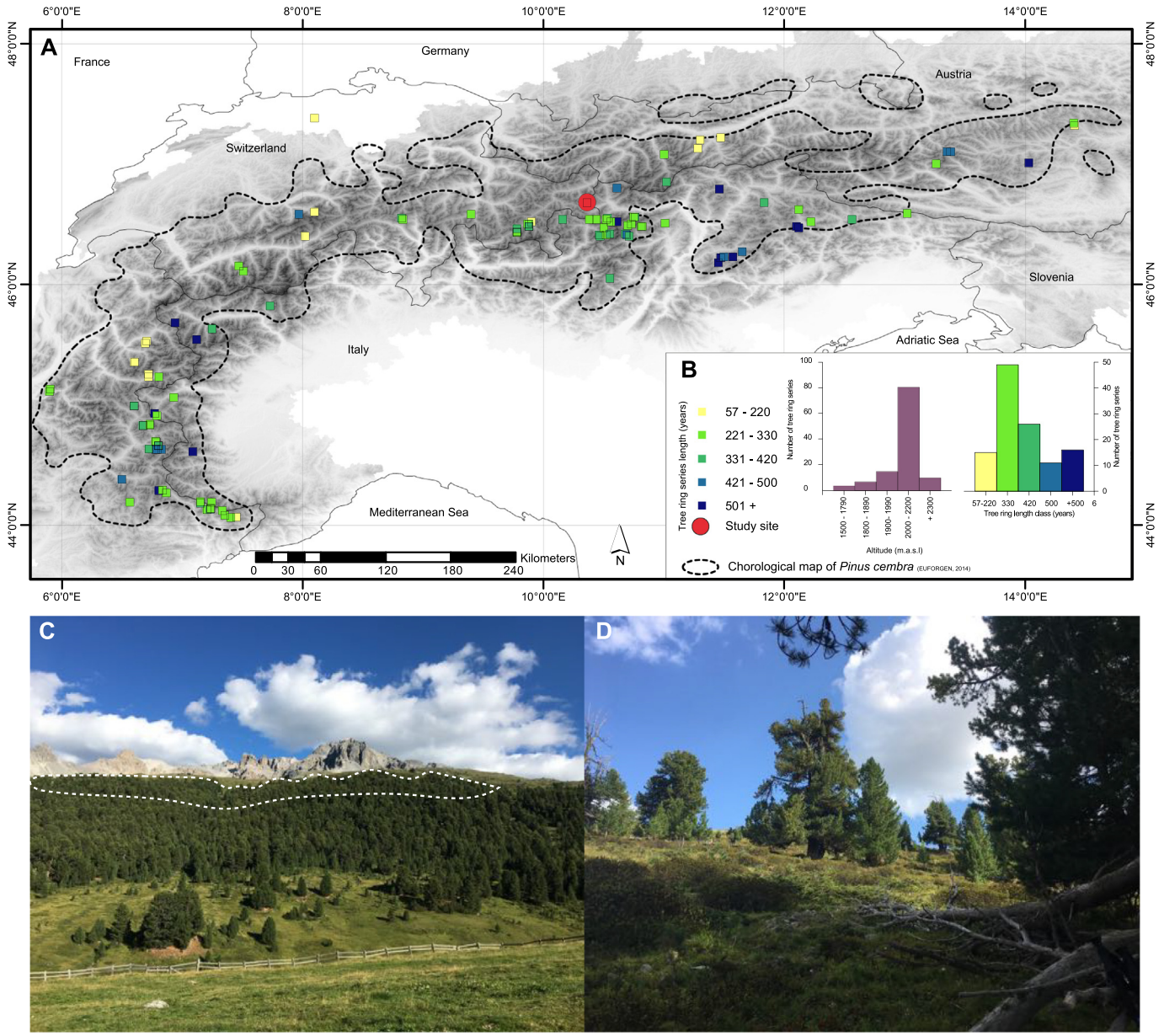

Fig. 1. (A) Network of published *Pinus cembra* L. chronologies from the European Alps based on an extensive literature survey. (B) Inset map: Material of most *P. cembra* chronologies was collected at treeline sites (>2000 m asl) and mean chronology lengths exceed 300 years. (C) Samples from this study originate from *God da Tamangur* (Val S-charl, Scuol, Grisons, Switzerland), the sampling site is indicated with a dashed white line. (D) Detailed view of a century-old *P. cembra* tree selected for analysis.

Table 1
Overview of dendroclimatic studies from the European Alps based on *Pinus cembra* L. and correlations obtained with precipitation (P) and temperature (T) records. Positive correlations are shown in red, negative correlations in blue.

Reference	Sep	Oct	Nov	Dec	Jan	Feb	Mar	Apr	May	Jun	Jul	Aug	Sep	Significance	Type
Carrer and Urbinati, 2004										P	T			r/s 4.2 r/s -3.8	TRW
Oberhuber 2004	T						T P				T			*r* 0.3 ; *r* -0.3 *r* 0.3	TRW
Franck et al., 2005										T	T	T		*r* 0.4	TRW - MXD
Leal et al., 2007										T	T			*r* -0.39	TRW
Carrer et al., 2007	T	T	T	T P	P		T		T	T	T	T		r/s 4-5 ; r/s -2.3 r/s 4	TRW
Esper et al., 2008										T	T	T		*r* 0.4	TRW
Oberhuber et al., 2008	T P	T	P				T			T	T			*r* 0.3 *r* 0.25	TRW
Vittoz et al., 2008		P	T								T			- -	TRW
Leonelli et al., 2009	P	P	P							T	T	T		*r* 0.38 *r* 0.25	TRW
Popa and Kern, 2009										T	T	T		*r* 0.6	TRW
Carrer, 2011	T	T	T	T						T	T			r/s 6	TRW
Saulnier et a., 2011				P			T			T	T			*r* -0.2 ; *r* 0.2 *r* 0.2	TRW
Carrer et al., 2018										T	T	T		*r* 0.5	QWA
Cerrato et al., 2019											T	T	T	*r* 0.6	MXD

limit its suitability for climatic reconstructions based on MXD (Schweingruber and Johnson, 1993; Schweingruber, 1985), a finding that was confirmed more recently by Frank et al. (2005), showing that correlations between MXD and climate were consistently lower than those found in other widespread Alpine conifer species.

Quantitative wood anatomy (QWA) – defined as the analysis of the variability of xylem anatomical features along dated tree-ring series – could alleviate this problem (Von Arx et al., 2016; Björklund et al., 2019) as it operates at the cellular level, analyzes a wide number of anatomical parameters (i.e. lumen area, lumen diameter, cell wall-thickness) and showcases a strong summer temperature signals of latewood cell wall thickness (Carrer et al., 2017; Björklund et al., 2020; Seftigen et al., 2022). Following studies by Carrer et al. (2018) in the Italian Alps and Știrbu et al. (2022) in the Carpathians, showing significant correlation between cell wall thickness and summer temperatures, we hypothesize that QWA could offer an alternative to MXD series to trace past temperature variability from *P. cembra* trees.

In this study, we therefore employ QWA with the objective to test the suitability of *P. cembra* series for climate reconstruction. Using increment cores from trees growing in the highest continuous and one of the oldest *P. cembra* forests of the European Alps, we (i) construct chronologies for four different wood anatomical parameters (i.e. tangential and radial cell wall thickness, cell lumen area and anatomical MXD); (ii) quantify climate-tree growth relations by contrasting daily meteorological records from the E-OBS dataset and the QWA chronologies; so as to (iii) test correlation robustness and suitability of *P. cembra* QWA series with a calibration-verification procedure.

2. Material and methods

2.1. Study site

Our study site is located in *God da Tamangur* (46.68°N; 10.36°E) – meaning the « forest back there» in Vallader Romansch – known as the highest, pure, and continuous *P. cembra* forest in Europe (Fig. 1A, C, D). The forest is located at an elevation of up to 2300 m asl, at the furthest end of the Val S-charl, south of Scuol, Grisons, Switzerland, on the NW-facing slope of Piz Starlex (3075 m asl). Due to its remote location and high elevation, the forest has been spared from massive logging which was quite widespread in the valley because of intense mining activities. To the Romansch culture and language, the Tamangur forest has become a symbol of tenacity, strength and also symbolizes the will to survive. The forest nature reserve *God da Tamangur* stretches across 86 ha (Fig. 1C). Annual mean temperature and precipitation sums measured at the Buffalora meteorological station (1968 m asl), located 7.6 km SW from our study site, amount to 5.75 °C and 677 mm, respectively (Meteo Swiss, 2022).

2.2. Sample collection and wood processing

Samples were collected during two field campaigns in summer 2017 and 2018. During the first campaign and with the purpose to build a robust TRW chronology, we sampled 45 long-lived *P. cembra* trees, growing between 2100 and 2300 m asl, without any visible faults such as nodes, reaction wood, or rotten parts. From each tree we extracted two increment cores at breast height (at ca. 130 cm above ground). Ring widths were measured to the nearest 0.01 mm using TSAPWin (Rinntech, Germany), crossdated using standard dendrochronological procedures (Stokes and Smiley, 1968) and checked for dating and measurement errors with the COFECHA software (Holmes, 1983). Based on the preliminary analyses of the tree-ring width series, we selected 9 individual trees showing the best inter-series correlation and covering the period 1920–2017. To perform wood cell anatomical measurements, these trees were sampled in summer 2018 using a 12 mm increment borer. The 12 mm cores were split into 4–5 cm long pieces to obtain 15-μm-thick cross-section with a Rotary Microtome (Leica RM 2255/2245). The sections were stained with Safranin and Astra blue to increase contrast and fixed with Canada balsam following standard protocols (Gärtner and Schweingruber, 2013; von Arx et al., 2016). Digital images of the microsections - at a resolution of 2.27 pixels/μm - were produced at the Swiss Federal Research Institute WSL (Birmensdorf, Switzerland), using a Zeiss Axio Scan Z1 (Carl Zeiss AG, Germany).

2.3. Wood anatomical measurements and chronology statistics

For the 9 selected trees, we used the ROXAS (v3.1) image analysis software (von Arx and Carrer, 2014) to automatically detect anatomical structures for all tracheid cells and annual ring boundaries for the period 1920–2017. We excluded measurements of samples with cell walls damaged during sampling or preparation. The output was summarized for four cell anatomical parameters (Fig. 2), including cell lumen area (LA), cell wall thickness oriented in radial (CWT_{rad}) and tangential (CWT_{tan}) directions (Prendin et al., 2017; Von Arx and Carrer, 2014) as well as anatomical maximum latewood density (aMXD) representing the maximum ratio between the cell wall area and the total cell area (the sum of cell wall and cell lumen area) throughout the ring (Björklund et al., 2020; Edwards et al., 2022). In addition, and with the goal to compare our findings with conventional tree-ring widths analyses, we also established a ring width (TRW) chronology.

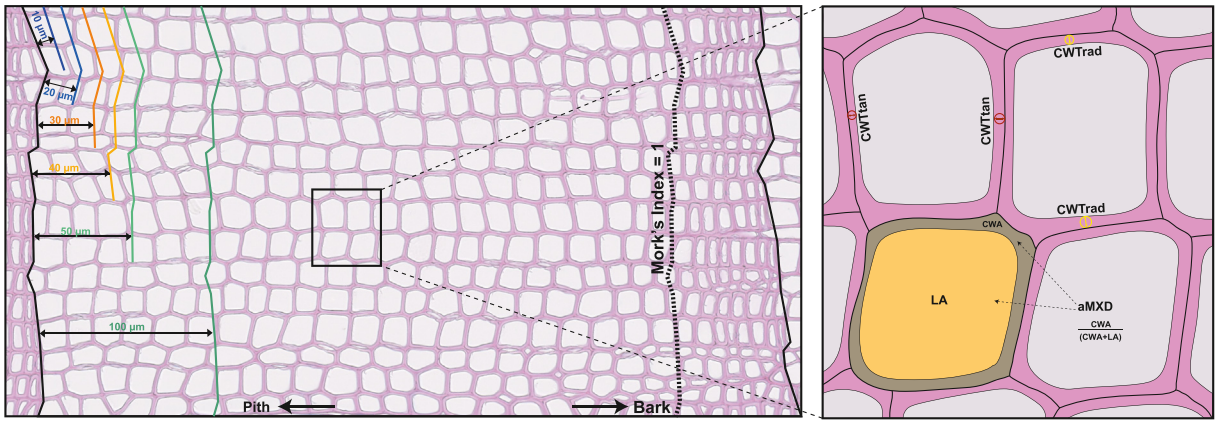

Fig. 2. Illustration of wood anatomical parameters analyzed in this study: CWT_{rad} – radial cell wall thickness, CWT_{tan} – tangential cell wall thickness, aMXD – anatomical maximum latewood density, CWA – cell wall area, LA – cell lumen area. The colored (blue to green) lines indicate different radial band widths (i.e. 10, 20, 30, 40, 50 and 100 µm) considered for the analysis of wood anatomical parameters. The dotted black line shows the transition between earlywood and latewood.

For each cell for which measurements were performed, we recorded the absolute and relative positions within each dated tree ring (Prendin et al., 2017; von Arx and Carrer, 2014). Following Björklund et al. (2020), we assigned each cell to tangential bands varying between 10 and 100 µm in radial width (with distances measured parallel to ring boundaries). In addition, we determined the transition from earlywood to latewood cells for each ring using Mork's index = 1 at a 10 µm radial resolution (Denne, 1988). For each ring, maximum values of CWT_{tan}, CWT_{rad} and aMXD were extracted from the bands identified as belonging to the latewood. For LA, maximum values were extracted from each ring irrespective of their position within earlywood or latewood.

The conventional ring-width measurements were detrended with a negative exponential function so as to eliminate non-climatic (e.g., age-related growth trends and other biological disturbances) effects from the series (Fritts, 1976; Cook and Kairiukstis, 1990). The detrended series were then aggregated into a TRW chronology using a biweight robust mean which reduces the influence of outliers (Cook and Peters, 1981). Given the absence of any evident long-term ontogenetic trend in anatomical series, detrending is not normally considered necessary (Carrer et al., 2018) in QWA studies. Yet, to increase interannual climatic signal and to remove multi-decadal trends in wood anatomical and meteorological time series, we standardized time series using a 30-year cubic smoothing spline, in addition to raw series. In a next step, empirical measures of dendroclimatic signals (Hughes et al., 2011) - average inter-series correlation ($RBAR_{EFF}$) and expressed population signal (EPS) (Wigley et al., 1984) - were computed to test the strength of the environmental information embedded in the chronologies using the maximum overlap of pairwise correlations (Bunn et al., 2014). All analyses were performed in R Studio (RStudio Team, 2020) using the R package dplR (Bunn, 2008; Bunn et al., 2014).

2.4. Assessing climate influence on tree-ring width and wood anatomical parameters

QWA data were correlated with the gridded (0.1° × 0.1° lat/long) E-OBS daily temperature dataset (Cornes et al., 2018). We selected the four grid-points centered over the sampling site (46.6–46.7° N; 10.3–10.4°E) and retrieved data for the period 1920–2017. Monthly temperatures from the E-OBS dataset are significantly correlated ($r > 0.87$, $p < 0.01$) with the meteorological series of Buffalora over the 1920–2017 period. For the growing season (April–September; or A-S) and summer (June–August; JJA) period, both meteorological series are correlated at 0.95 ($p < 0.01$).

To test for the robustness of the newly developed QWA series for dendroclimatic reconstructions, records (TRW and QWA) were scaled against the E-OBS dataset. We preferred scaling over regression to avoid artificial variance reduction (Esper et al., 2005). In addition and to go beyond the conventional monthly climate data aggregation (Fonti et al., 2010) and striving for a higher detail in the resolution of the most important associations, we calibrated regression models on temperatures averaged over one-to-365-days windows starting on January 1 of the year preceding ring formation (n-1) and ending on December 31 of the year in which the ring was formed (n) using the R package dendroTools (Jevšenak and Levanič, 2018). For each *P. cembra* parameter and optimal temperature time window identified from climate-growth relationships (see above), we computed 10,000 temperature reconstructions using a split calibration–verification procedure coupled with a bootstrap approach in which 50 % of the years covered by both the meteorological and tree-ring datasets were randomly extracted for calibration while the remaining years were used for validation over the 1920–2017 period. For each sampling, the root mean-square error (RMSE), coefficient of determination (r^2 for the calibration and R^2 for the verification periods), reduction of error (RE) and coefficient of efficiency (CE) statistics (Cook et al., 1995) were applied to test the predictive capacity of the transfer function. Calibration and validation statistics are illustrated for each parameter with their 5th, 50th and 95th percentiles.

3. Results

3.1. Chronology characteristics

We measured wood anatomical features for the period 1920–2017 CE on all samples for a total of 75–100 radial files per ring, with anatomical information catalogued by its position in each dated tree ring. After the exclusion of cells with walls damaged during sampling or preparation, a total of 1,393,924 tracheid cells were measured over the period 1920–2017.

Fig. 3 showcases the evolution of wood anatomical parameters as a function of relative distance to ring border. Based on Mork's index, we observe that latewood represents roughly 10 % of the ring width on average. *P. cembra* trees feature the classical ring structure of conifers growing in cold, temperate environments, with a monotonic reduction in cell lumen area (LA) on the one hand and an increase in cell wall thickness (CWT) and anatomical maximum latewood density (aMXD) from earlywood to latewood on the other hand. These trends differ just at the start of a ring for LA, with an evident increase at the very first part, and for tangential and radial CWT in latewood, showing a reduction at the end of the ring. We also observe that the peak of CWT_{rad} and aMXD is much more prominent than CWT_{tan} and best captured in radial band widths ranging from 10 to 40 µm.

The statistical characteristics of the Tamangur chronologies are summarized in Table 2. The EPS and Rbar values show that TRW has a stronger common signal (Rbar = 0.39, EPS = 0.85) than the wood anatomical chronologies (LA, CWT_{tan}, CWT_{Trad} and aMXD), with the Rbar for the latter ranging between 0.10 (for LA at 10 µm radial band width) and 0.34 (for a

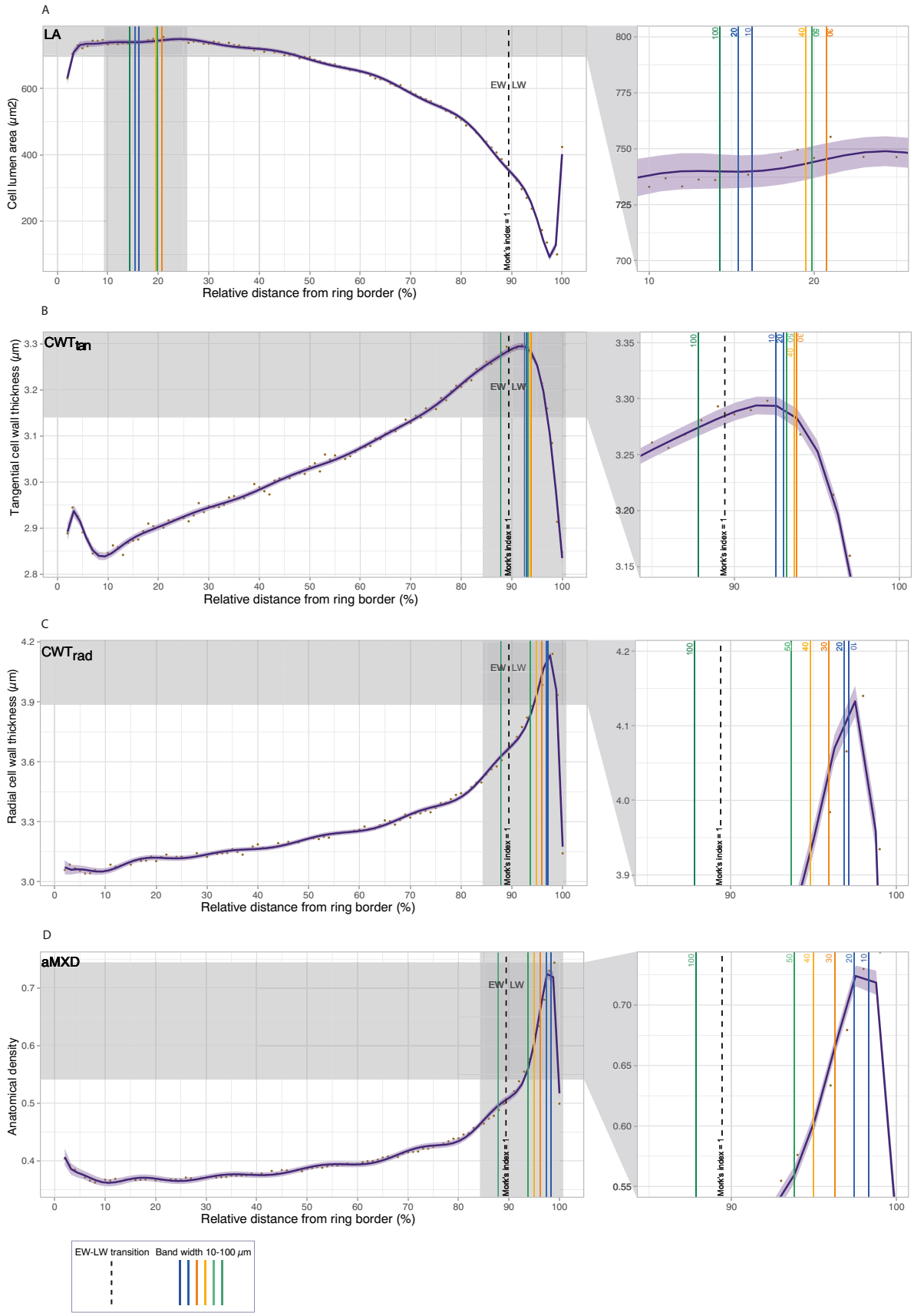

Fig. 3. Profile for (A) cell lumen area (LA), (B) tangential cell-wall thickness (CWT_{tan}), (C) radial (C) cell-wall thickness (CWT_{rad}) and (D) anatomical maximum latewood density (aMXD) along *Pinus cembra* tree rings. Black lines represent the mean values of nine trees over 97 years (1920–2017), whereas the violet shadowed areas delimit the 95 % confidence interval. Colored lines (from green to blue) represent the maximum values for each of the wood parameters analyzed for radial band widths ranging from 10 to 100 μm. The dotted black line shows the mean relative position of the transition between earlywood and latewood according to Morck's index = 1.

CWT_{Trad} at 30 μm radial band width; Table 2). The QWA parameter correlating best with TRW over the period 1920–2017 is LA with correlations ranging from 0.37 (for a radial band width of 20 μm) to 0.44 (for a radial band width of 10 μm). Correlations between TRW and CWT_{tan}, CWT_{rad} and aMXD are only slightly lower with a range going from 0.31 (for aMXD with a radial band width of 10 μm) to 0.41 (for CWT_{rad} with a radial band width of 30 μm).

3.2. Climate-growth relationships

Correlation coefficients between different tree-ring width and wood anatomical parameters with daily climate data retrieved from E-OBS over the period 1920–2017 point to temperature as the main driver of growth, yielding positive and significant values for both TRW and QWA parameters. By contrast, much weaker, mostly non-significant correlations can be found with precipitation (not shown).

Table 2 provides key insights into the time windows for which temperatures can best explain *P. cembra* growth. All statistics provided in the following are for correlations between raw data of anatomical traits and temperature data. For LA, the best correlation ($r = 0.56$; $p < 0.05$) is found with temperatures from May 20 to September 6 (109 days) occurred in the year preceding ring formation (n-1) for a radial band width of 20 μm. Considerably higher correlations are obtained for the various QWA chronologies, namely between CWT_{tan} (10 μm radial band width) and aMXD (20 μm radial band width) with temperatures for the time windows comprised between May 14 and September 4 (113 days; $r = 0.71$, $p < 0.05$) and July 15 and August 30 (46 days; $r = 0.74$, $p < 0.05$), respectively. The highest correlations are obtained between the CWT_{rad} chronology and temperatures over a 130-day time window centered between April 30 and September 7 ($r = 0.79$; $p < 0.05$). If the period considered is restricted to the period 1950–2017 for which the E-OBS network is considered very robust by the data providers, we even obtain a correlation of $r = 0.87$ ($p < 0.05$). Noteworthy, correlation between this last wood anatomical parameter and the time window of air temperatures considered varies only very little (i.e. comprised between $r = 0.76$ to 0.79 and time windows fluctuating only between April 26 to May 2 for the start and September 7 to 9 for the end dates) irrespective of the radial band width selected for analysis.

In the case of detrended time series, correlations are systematically lower compared to those obtained for raw data. In the case of TRW, for which only a detrended chronology could be analyzed, the highest correlation with temperature is obtained for a fairly long time window of 118 days comprised between March 8 and July 4 ($r = 0.57$; $p < 0.05$). In the case of CWT_{rad}, detrending results in lower, yet very significant correlations between temperatures and different CWT_{rad} chronologies with values ranging between $r = 0.57$ ($p < 0.05$; 10 μm radial band width) and 0.66 ($p < 0.05$; 40 μm radial band width).

3.3. Calibration and verification statistics

Table 2 evidences that the TRW and LA reconstructions are poorly robust with a RE of 0.13 [−0.33 to 0.39] and 0.1 [−0.4 to 0.35] as well as a CE of 0.09 [−0.39 to 0.38] and 0.07 [−0.49 to 0.32] for TRW and LA (at 20 μm), respectively. Much more robust reconstructions are obtained for the CWT_{tan} (10 μm) and aMXD (20 μm) with RE of 0.39 and 0.46 as well as a CE of 0.37 and 0.44, respectively. These statistics remain systematically positive irrespective of the year extracted during the bootstrap sampling. Again, the best results are obtained with CWT_{rad} (40 μm) with a RE = 0.57 [0.37 to 0.69] and a CE = 0.55 [0.34 to 0.67], thus pointing to a significant and considerable skill in estimating mean air temperature from April 30 to September 7.

Table 2
Statistics of reconstructions based on LA, CWT_{tan}, CWT_{rad}, aMXD and TRW for radial band widths ranging from 10 to 100 μm as well as optimal time windows used in reconstructions. EPS = expressed population signal, Rbar = average inter-series correlation, RMSE = root mean-square errors, r = coefficient of correlation, RE = reduction of error, CE = coefficient of efficiency. For details see text.

Band width (micron)	EPS	Rbar	RMSE	r	RE	CE	Time window
				LA			
10	0.479	0.102	0.895	[0.43–0.66] 0.55	[−0.36–0.33] 0.08	[−0.45–0.29] 0.05	5/27–7/28 (Prev.year)
20	**0.574**	**0.143**	**0.878**	[0.45–0.66] **0.56**	[−0.4–0.35] **0.1**	[−0.49–0.32] **0.07**	**5/20–9/06** (Prev.year)
30	0.581	0.146	0.974	[0.4–0.61] 0.51	[−0.54–0.55] 0	[−0.63–0.22] -0.03	5/26–7/22 (Prev.year)
40	0.608	0.161	0.97	[0.4–0.62] 0.51	[−0.5–0.26] 0.01	[−0.58–0.23] -0.03	5/26–7/30 (Prev.year)
50	0.605	0.16	0.991	[0.38–0.61] 0.5	[−0.56–0.25] -0.02	[−0.65–0.21] -0.05	5/27–7/28 (Prev.year)
100	0.609	0.161	0.96	[0.41–0.62] 0.51	[−0.52–0.27] 0.01	[−0.6–0.24] -0.02	5/26–7/20 (Prev.year)
				CWTTAN			
10	**0.636**	**0.178**	**0.584**	[0.61–0.79] **0.71**	[0.12–0.56] **0.39**	[0.07–0.54] **0.37**	**5/14–9/08**
20	0.661	0.195	0.61	[0.59–0.77] 0.69	[0.1–0.54] 0.37	[0.05–0.52] 0.35	4/08–9/08
30	0.623	0.171	0.611	[0.59–0.77] 0.69	[0.02–0.55] 0.37	[−0.02–0.53] 0.34	5/12–9/08
40	0.632	0.177	0.647	[0.56–0.76] 0.67	[0.03–0.49] 0.32	[−0.01–0.46] 0.3	4/08–9/08
50	0.61	0.164	0.731	[0.51–0.73] 0.63	[−0.06–0.43] 0.24	[−0.11–0.4] 0.21	4/07–9/08
100	0.567	0.147	0.753	[0.49–0.74] 0.62	[−0.13–0.43] 0.22	[−0.18–0.41] 0.19	5/17–9/06
				CWTRAD			
10	0.783	0.31	0.471	[0.68–0.83] 0.76	[0.3–0.64] 0.51	[0.26–0.62] 0.49	5/20–9/07
20	0.799	0.332	0.44	[0.7–0.84] 0.78	[0.33–0.67] 0.54	[0.29–0.66] 0.52	4/28–9/07
30	0.805	0.339	0.422	[0.72–0.85] 0.79	[0.36–0.69] 0.56	[0.33–0.67] 0.54	4/30–9/08
40*	**0.801**	**0.335**	**0.416**	[0.72–0.85] **0.79**	[0.37–0.69] **0.57**	[0.34–0.67] **0.55**	**4/30–9/07**
50	0.795	0.328	0.421	[0.72–0.85] 0.79	[0.37–0.68] 0.56	[0.34–0.66] 0.54	4/30–9/07
100	0.769	0.307	0.418	[0.73–0.84] 0.79	[0.38–0.67] 0.57	[0.35–0.66] 0.55	4/26–9/09
				aMXD			
10	0.665	0.198	0.595	[0.62–0.77] 0.7	[0.04–0.57] 0.39	[0–0.55] 0.36	7/15–8/30
20	**0.663**	**0.197**	**0.522**	[0.66–0.8] **0.74**	[0.14–0.63] **0.46**	[0.1–0.61] **0.44**	**7/15–8/30**
30	0.702	0.227	0.595	[0.61–0.78] 0.7	[0.04–0.58] 0.39	[0–0.56] 0.37	7/15–9/04
40	0.707	0.232	0.605	[0.61–0.77] 0.7	[0.06–0.54] 0.38	[0.02–0.53] 0.35	4/11–10/06
50	0.702	0.229	0.644	[0.59–0.74] 0.68	[−0.01–0.51] 0.34	[−0.06–0.49] 0.31	4/12–10/06
100	0.606	0.17	0.772	[0.49–0.71] 0.61	[−0.19–0.42] 0.21	[−0.24–0.39] 0.17	7/15–8/20
				RW			
	0.85	0.39	0.84	[0.27–0.53] 0.41	[−0.85–0.16] -0.2	[−0.93–0.13] -0.26	7/15–8/08

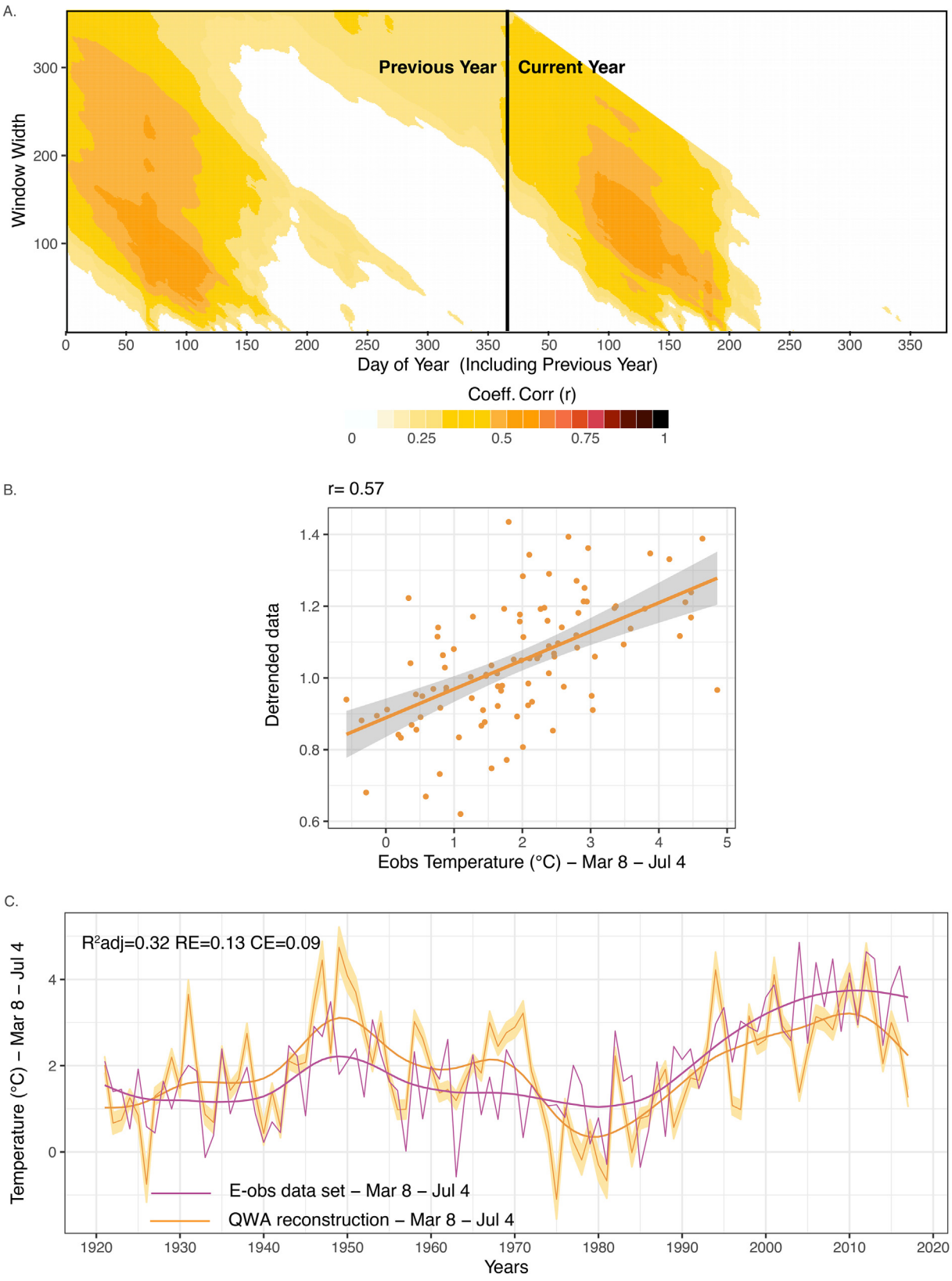

Fig. 4. (A) Correlations of the spline detrended ring widths (TRW) chronology and E-OBS air temperatures over time windows ranging from 1 to 365 days. (B) Regression between detrended TRW data and E-OBS air temperature for a time window extending from March 8 to July 4 for which correlations ($r = 0.57$) were found to be highest. (C) Comparison of interannual and decadal (i.e. smoothed with a 11-yr spline) E-OBS and TRW reconstructed air temperatures for a time window extending from March 8 to July 4 over the period 1920–2017.

3.4. Temperature reconstruction

Based on the above statistics, Fig. 4 presents the temperature reconstruction based on a conventional TRW chronology for which *P. cembra* has hitherto been shown to provide only poorly significant results. The graph shows reconstructed air temperatures from March 8 to July 4 computed as the median of 10,000 realizations given with the 95 % bootstrap confidence interval and compared to the E-OBS dataset over the period 1920–2017. At interannual timescales, the reconstruction underestimates temperatures at several instances, with the most notable differences observed in 2004 (underestimation of − 2.85 °C), 1975 (−1.78 °C) and 1987 (−0.68 °C). By contrast, the reconstruction also overestimates air temperatures in a considerable manner, namely in 1949 (overestimation of +2.4 °C) and 1971 (+2.36 °C). Over the period 1920–2017, the RMSE computed between the observed and TRW reconstructed air temperatures is 0.84. At decadal timescales, the adjusted coefficient of determination between the 11-year spline smoothed observed and reconstructed temperatures is $r(adj)^2 = 0.55$, yet the TRW-based reconstruction overestimates air temperatures over the periods 1945–1954 and 1963–1972 by +0.8 and + 0.85 °C, respectively. At the same time, it fails to reproduce the anthropogenic warming as observed in the instrumental records since at least the mid-1990s.

Fig. 5 provides the best reconstruction obtained from wood anatomical parameters, that is a reconstruction based on a raw, non-detrended CWT_{rad} chronology and a radial band width of 40 μm. We show reconstructed air temperatures from April 30 to September 7 computed as the median of 10,000 realizations given with the 95 % bootstrap confidence interval and compared to the E-OBS dataset over the period 1920–2017. At interannual timescales, the RMSE is much better than that obtained for TRW with 0.42, with a maximum discrepancy between the observed and reconstructed air temperatures during the heatwave of 2003 (with the recorded temperatures exceeding the reconstructed values by +1.8 °C) and during the 1930s, for which the reconstruction overestimates air temperatures by roughly 1.4 °C in 1932, 1933 and 1939. At decadal timescales, the $r(adj)^2$ between observed and reconstructed air temperatures is 0.85. Whereas the raw, non-detrended CWT_{rad} chronology also captures the recent warming adequately, it overestimates observed temperatures by 0.7 °C over the 1925–1934 period.

4. Discussion

4.1. Statistical quality of the chronologies

In this study, we use *P. cembra* tree-ring and wood anatomical parameters to test the suitability of the species for robust temperature reconstructions. By contrast to previous work, where the potential of this very widespread, timberline-forming species has been considered to be too weak (Schweingruber, 1985), we demonstrate that wood anatomical parameters, and especially radial cell wall thickness (CWT_{rad}), can indeed serve as very promising and accurate proxies to reconstruct past summer air temperatures. These findings do not only bring *P. cembra* back to the spotlight of dendroclimatic research, but also opens new perspective in paleoclimatology as the species is very long-lived, abundant at high elevations (Carrer et al., 2018, Fig. 1A) and was sampled extensively in the past with >120 chronologies existing to date.

Similarly, we call for more wood anatomical chronologies of *P. cembra* to be built as they represent suitable proxies for climate reconstruction in the Alps provided that (1) correlations among series is high (Fonti and García-Gonzalez (2008), (2) the climatic fingerprint in series of anatomical parameters is stronger and less noisy than the signal found in TRW (García-González et al., 2016) and (3) that the wood anatomical reconstructions pass the calibration/verification statistics. In this work, and as frequently reported in other studies (Balanzategui et al., 2021; Ziaco et al., 2016), inter-series correlation for the wood anatomical parameters are lower than those found for TRW. They exceed the values reported by Carrer et al. (2016) for spruce (0.13) and larch (0.18) trees in the Alps and are comparable to those (0.23 for CWT_{tan}, 0.24 for CWT_{rad}) reported for *P. cembra* in the Carpathians (Știrbu et al., 2022). The weaker empirical signal strength that we observe in chronologies built from CWT_{tan}, CWT_{rad} and aMXD could be explained by the heterogeneity induced by intra-annual biological processes controlling carbon assimilation and allocation in tree rings (Eilmann et al., 2006; Fonti and García-González, 2004).

4.2. Suitability of wood anatomical parameter series for climate reconstruction in the Alps

Our study confirms the limited suitability of TRW chronologies of *P. cembra* for climate reconstructions (Schweingruber, 1985) and corroborates that one should refrain from reconstructing climate using *P. cembra* TRW chronologies (Fig. 4). By contrast, we find highly significant, positive correlations between CWT_{rad} (with a radial band width of 40 μm) and mean air temperatures. Interestingly, the period for which the highest correlations are obtained matches closely with the assumed length of the vegetation period at the study site (end of April to early-September; Fig. 5; Gruber et al., 2018). Our findings agree with Carrer et al. (2018) stating that correlations >0.6 could be obtained between *P. cembra* CWT_{rad} measured in earlywood cells and June temperatures as well as between CWT_{rad} measured in latewood cells and August temperatures. They are also in line with Știrbu et al. (2022) who reported significant correlation ($r = 0.65$ over the 1961–2013 period) between CWT chronologies of *P. cembra* and summer (JJA) temperatures. The correlations obtained for God da Tamangur exceed those (r = 0.6) reported for the Upper Val di Pejo (Italian Alps) MXD chronology, located 40 km SE of God da Tamangur, and summer (JJA) air temperatures over the period 1901–2015 (Cerrato et al., 2019). When comparing our results to reconstructions based on MXD chronologies of L. *decidua*, our CWT_{rad} reconstruction reaches values ($r = 0.79$ and CE = 0.55 for the period 1920–2017) that exceed those reported in one of the most widely used European Alps temperature proxy records (Büntgen et al., 2006; $r = 0.73$ with a CE = 0.47 for the period 1911–2003). In the case of the smoothed reconstructions, a value of $r = 0.69$ (1818–2003) is computed between the 20-year smoothed MXD L. *decidua* chronology and the JJAS temperature from the Histalp dataset (Auer et al., 2007), whereas we obtain a correlation of $r = 0.9$ (0.92) between the 11- (20)-year smoothed CWT_{rad} chronology and the E-OBS dataset. Noteworthy, if the reconstruction of mean air temperatures is limited to 1950, correlation values even reach $r = 0.86$ and CE = 0.69. Such a limitation in time can be justified as the E-OBS dataset with daily temperature values still has a research status for the period 1920–1949 (i.e. the pre-1950 version) and is not updated regularly. The authors of the database state themselves that quality control has been minimal for the pre-1950 period and that station density is low, such that erroneous values cannot be excluded for data-poor areas like the Alps (Cornes et al., 2018). This may also explain to a certain extent the discrepancies found between the observed and reconstructed air temperatures, especially the systematic overestimation of reconstructed temperatures between the 1920s and the late 1930s, as well as the extremes observed in 1932, 1933, and 1939.

4.3. Wood anatomical reconstructions of P. cembra – a new gold standard in Alpine dendroclimatology?

A major advantage of wood anatomical reconstructions based on long-lived *P. cembra* trees over classic TRW or MXD reconstructions is the fact that they are built from raw data, that is without undergoing any standardization procedures. This is in contrast to most reconstructions where standard individual-series detrending is applied to remove age trends (Cook et al., 1990; Lindholm and Eronen, 2000; Grudd et al., 2002). Yet, such a removal can be problematic as it limits the conservation of climatic information over periods equivalent to the mean segment length, a phenomenon described as the 'segment length curse' (Cook et al., 1995). Whereas approaches including the widely employed Regional Curve Standardization (Briffa et al., 1998; Esper et al., 2003; Briffa and Melvin, 2011; Melvin and Briffa, 2014) may offer significant improvements over traditional

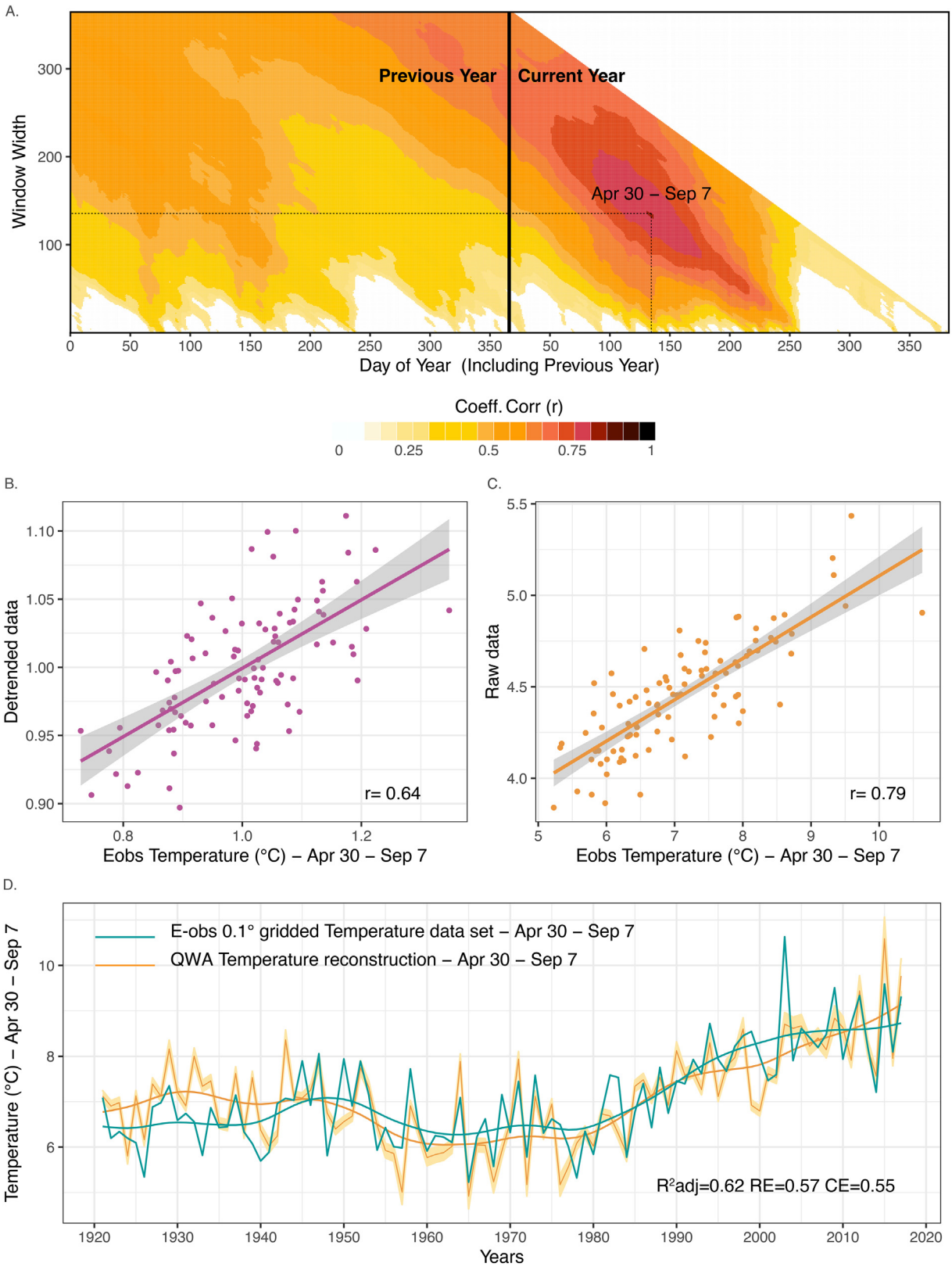

Fig. 5. (A) Correlations of the raw radial cell-wall thickness (CWT_{rad}) chronology and E-OBS air temperatures over time windows ranging from 1 to 365 days. (B) Regression between detrended CWT_{rad} data and E-OBS air temperature for a time window extending from April 30 to September 7 for which correlations ($r = 0.64$) were found to be highest. (C) Regression between raw CWT_{rad} data and E-OBS air temperature for a time window extending from April 30 to September 7 for which correlations ($r = 0.79$) were found to be highest. (D) Comparison of interannual and decadal (i.e. smoothed with a 11-yr spline) E-OBS and CWT_{rad} reconstructed air temperatures for a time window extending from April 30 to September 7 over the period 1920–2017.

detrending methods, this may be limited to datasets with high sample replication and heterogeneous age structure (Gagen et al., 2007). The fact that statistical detrending can be avoided is a great advantage as it ultimately allows reconstruction of low-frequency, long-term changes in past climate from trees (Carrer et al., 2017, 2018).

Another advantage of wood anatomical reconstructions is the lack of any divergence in the record (Cerrato et al., 2019), by contrast to the TRW chronology constructed at God da Tamangur or various TRW and MXD chronologies existing at other high-altitude / high-latitude sites (Jacoby and D'Arrigo, 1995; Carrer and Urbinati, 2006; D'Arrigo et al., 2008). At the same time, we also realize that none of the anatomical parameters analyzed is able to capture the amplitude of the heatwave of summer 2003 (Schär and Jendritzky, 2004). Should heatwaves like the ones recorded in summers 2003, 2009, 2011 or 2015 become the new normal (Perkins-Kirkpatrick and Lewis, 2020), it seems likely that even anatomical parameters will likely fail to record the trajectory of summer temperatures in the future (IPCC, 2019). In addition of potentially losing its ability to accurately record extremely warm summer temperatures, *P. cembra* could also find itself in the climate trap as the species could face difficulties to keep the pace with climate when it comes to adaptation to climate change (Dauphin et al., 2021).

The findings reported in this study clearly showcase the large potential of *P. cembra* for dendroclimatic purposes. Last but not least, it seems worthwhile to mention that *P. cembra* is a non-host species for the larch budmoth (LBM; Baltensweiler, 1993; Nola et al., 2006) which affects L. *decidua* trees cyclically (each 8–9 years; Baltenschweiler et al., 1977; Esper et al., 2007) to defoliate their needles. Insect defoliation thereby leads to markedly reduced ring increments and mass over two to five years (Kulman, 1971; Battipaglia et al., 2014; Arbellay et al., 2018; Castagneri et al., 2020) due to a reduction of the tree's photosynthetic capacity and the related suppression of tree growth due to lower carbon assimilation and the heavy reliance on carbohydrate reserves to replace foliage (Gleason and Ares, 2004; Myers and Kitajima, 2007). As a result, LBM outbreaks will largely suppress climate signals in L. *decidua* in such a way that TRW chronologies have been considered unsuitable for high-frequency reconstructions (Weidner et al., 2010). Likewise, the very low ring increments observed during LBM outbreaks (Schweingruber, 1979) have often been removed in MXD chronologies and densities were estimated with a gap filling procedure (Büntgen et al., 2006), leaving, however, considerable uncertainties in reconstructions. *P. cembra*, by contrast, has been used as a reference species to disentangle the effect of insect defoliation on TRW or MXD in L. *decidua* from that of adverse climatic conditions (Dormont et al., 2006; Büntgen et al., 2009). Our study shows that in addition to its potential to allow disentangling non-climatic effects in L. *decidua* chronologies, wood anatomical parameters of *P. cembra* clearly have the potential to yield highly valuable and solid chronologies of their own at annual to decadal timescales and for most parts of the European Alps due to their ubiquitous occurrence at treeline sites.

5. Conclusions

The wood anatomical chronologies based on *P. cembra* traits unveil a dormant potential and open new avenues for a species that has hitherto been considered unsuitable for climate reconstructions. By comparing wood anatomical parameters with daily temperature records, the wood anatomical approach also allows improving the quality of inferences compared to classical dendroclimatic approaches (TRW or MXD; Carrer et al., 2018), as the latter usually compare monthly temperature values with yearly ring widths or maximum latewood density. Findings of this paper – as well as those of Carrer et al. (2018) – are encouraging and call for further reconstructions based on *P. cembra* wood anatomical parameters. In addition, *P. cembra* could become a valuable addition or alternative to L. *decidua* reconstructions as they conserve decadal to multi-decadal climate variability without any detrending.

The construction of wood anatomical reconstructions has a cost and requires efforts that remain more substantial than what is currently needed for TRW or MXD reconstructions (Björklund et al., 2020). As the wood anatomical series of *P. cembra* represent a substantial of proxy data – and could not be obtained from ring widths or densities – the effort is nonetheless justified, especially as wood anatomical procedures are constantly improving and the need for fewer samples will likely render the approach more efficient and effective in the near future.

CRediT authorship contribution statement

Lopez-Saez Jérôme: Conceptualization, Methodology, Investigation, Writing-Original draft preparation. **Corona Christophe**: Conceptualization, Methodology, Software, Investigation, Writing-Original draft preparation. **von Arx Georg**: Software, Validation, Writing - Review & Editing. **Fonti Patrick**: Validation, Writing - Review & Editing. **Slamova Lenka**: Resources. **Stoffel Markus**: Supervision, Writing-Original draft preparation.

Data availability

The data that has been used is confidential.

Declaration of competing interest

The authors declare that they have no known competing financial interests or personal relationships that could have appeared to influence the work reported in this paper.

Acknowledgements

JLS, CC, and MS acknowledge support from the Swiss National Science Foundation (SNSF) Spark project "MNEMOSYNE" and a scnat research grant from the Research Commission of the Swiss National Park (FOK-SNP). C.C., P.F., J.L.-S. and M.S. received funding from the Swiss National Science Foundation (SNSF) Sinergia project CALDERA (no. CRSIIS_183571), whereas GvA was supported by the SNSF project XELLCLIM (grant no. 200021_182398).

References

Arbellay, E., Jarvis, I., Chavardès, R.D., Daniels, L.D., Stoffel, M., 2018. Tree- ring proxies of larch bud moth defoliation: latewood width and blue intensity are more precise than tree-ring width. Tree Physiol. 38, 1237–1245. https://doi.org/10.1093/treephys/tpy057.

von Arx, G., Carrer, M., 2014. ROXAS–a new tool to build centuries-long tracheid-lumen chronologies in conifers. Dendrochronologia 32, 290–293. https://doi.org/10.1016/j.dendro.2013.12.001.

von Arx, G., Crivellaro, A., Prendin, A.L., Cufar, K., Carrer, M., 2016. Quantitative wood anatomy-practical guidelines. Front. Plant Sci. 7. https://doi.org/10.3389/fpls.2016.00781.

Auer, I., Böhm, R., Jurkovic, A., Lipa, W., Orlik, A., Potzmann, R., Schöner, W., Ungersböck, M., Matulla, C., Briffa, K., Jones, P., Efthymiadis, D., Brunetti, M., Nanni, T., Maugeri, M., Mercalli, L., Mestre, O., Moisselin, J.-M., Begert, M., Muller-Westermeier, G., Kveton, V., Bochnicek, O., Stastny, P., Lapin, M., Szalai, S., Szentimrey, T., Cegnar, T., Dolinar, M., Gajic-Capka, M., Zaninovic, K., Majstorovic, Z., Nieplova, E., 2007. HISTALP – historical instrumental climatological surface time series of the Greater Alpine Region. Int. J. Climatol. 27, 17–46. https://doi.org/10.1002/joc.1377.

Balanzategui, D., Nordhauß, H., Heinrich, I., Biondi, F., Miley, N., Hurley, A.G., Ziaco, E., 2021. Wood anatomy of Douglas-fir in Eastern Arizona and its relationship with Pacific Basin climate. Front. Plant Sci. 12, 702442. https://doi.org/10.3389/fpls.2021.702442.

Baltenschweiler, W., Benz, G., Bovey, P., Delucchi, V., 1977. Dynamics of larch bud moth populations. Annu. Rev. Entomol. 22 (1), 79–100.

Baltensweiler, W., 1993. Why the larch bud moth cycle collapsed in the subalpine larch-cembran pine forests in the year 1990 for the first time since 1850. Oecologia 94, 62–66. https://doi.org/10.1007/BF00317302.

Battipaglia, G., Büntgen, U., McCloskey, S.P.J., Blarquez, O., Denis, N., Paradis, L., 2014. Long-term effects of climate and land-use change on larch budmoth outbreaks in the French Alps. Clim. Res. 62, 1114. https://doi.org/10.3354/cr01251.

Björklund, J., von Arx, G., Nievergelt, D., Wilson, R., Van den Bulcke, J., Günther, B., Loader, N.J., Rydval, M., Fonti, P., Scharnweber, T., Andreu-Hayles, L., Büntgen, U., D'Arrigo, R., Davi, N., De Mil, T., Esper, J., Gärtner, H., Geary, J., Gunnarson, B.E., Hartl, C., Hevia, A., Song, H., Janecka, K., Kaczka, R.J., Kirdyanov, A.V., Kochbeck, M., Liu, Y., Meko, M., Mundo, I., Nicolussi, K., Oelkers, R., Pichler, T., Sánchez-Salguero, R., Schneider, L., Schweingruber, F., Timonen, M., Trouet, V., Van Acker, J., Verstege, A., Villalba, R., Wilmking, M., Frank, D., 2019. Scientific merits and analytical challenges of tree-ring densitometry. Rev. Geophys. 57, 1224–1264. https://doi.org/10.1029/2019RG000642.

Björklund, J., Seftigen, K., Fonti, P., Nievergelt, D., von Arx, G., 2020. Dendroclimatic potential of dendroanatomy in temperature-sensitive Pinus sylvestris. Dendrochronologia 60, 125673. https://doi.org/10.1016/j.dendro.2020.125673.

Briffa, K.R., Melvin, T.M., 2011. A closer look at regional curve standardization of tree- ring records: justification of the need, a warning of some pitfalls, and suggested improvements in its application. Dendroclimatology. Springer, Dordrecht, pp. 113–145.

Briffa, K.R., Schweingruber, F.H., Jones, P.D., Osborn, T.J., Shiyatov, S.G., Vaganov, E.A., 1998. Reduced sensitivity of recent tree-growth to temperature at high northern latitudes. Nature 391, 678–682.

Bunn, A.G., 2008. A dendrochronology program library in R (dplR). Dendrochronologia 26, 115–124. https://doi.org/10.1016/j.dendro.2008.01.002.

Bunn, A.G., Korpela, M., Biondi, F., Campelo, F., Mérian, P., Mudelsee, M., et al., 2014. "dplR: Dendrochronology Program Library in R". R Package Version 1.5.9. Available at http://CRAN.R-project.org/package=dplR.

Büntgen, U., Esper, J., Franck, D.C., Nicolussi, K., Schmidhalter, M., 2005. A 1052-year tree-ring proxy for Alpine summer temperatures. Clim. Dyn. 25, 141–153. https://doi.org/10.1007/s00382-005-0028-1.

Büntgen, U., Bellwald, I., Kalbermatten, H., Schmidhalter, M., Frank, D.C., Freund, H., Bellwald, W., Neuwirth, B., Nüsser, M., Esper, J., 2006. 700 years of settlement and building history in the LötschentalSwitzerland. Erdkunde 96–112.

Büntgen, U., Frank, D., Liebhold, A., Johnson, D., Carrer, M., Urbinati, C., Grabner, M., Nicolussi, K., Lavanic, T., Esper, J., 2009. Three centuries of insect outbreaks across the European Alps. New Phytol. 182, 929–941. https://doi.org/10.1111/j.1469-8137.2009.02825.x.

Carrer, M., 2011. Individualistic and time-varying tree-ring growth to climate sensitivity. PLoS One 6 (7), e22813. https://doi.org/10.1371/journal.pone.0022813.

Carrer, M., Urbinati, C., 2004. Age-dependent tree-ring growth responses to climate in Larix decidua and Pinus cembra. Ecology 85, 730–740. http://www.jstor.org/stable/3450399.

Carrer, M., Urbinati, C., 2006. Long-term change in the sensitivity of tree-ring growth to climate forcing in Larix decidua. New Phytol. 170, 861–871. https://doi.org/10.1111/j.1469-8137.2006.01703.x.

Carrer, M., Nola, P., Eduard, J.L., Motta, R., Urbinati, C., 2007. Regional variability of climate-growth relationships in Pinus cembra high elevation forests in the Alps. J. Ecol. 95 (5), 1072–1083. https://doi.org/10.1111/j.1365-2745.2007.01281.x.

Carrer, M., Brunetti, M., Castagneri, D., 2016. The imprint of extreme climate events in century-long time series of wood anatomical traits in high-elevation conifers. Front. Plant Sci. 7. https://doi.org/10.3389/fpls.2016.00683.

Carrer, M., Castagneri, D., Prendin, A.L., Petit, G., von Arx, G., 2017. Retrospective analysis of wood anatomical traits reveals a recent extension in tree cambial activity in two high-elevation conifers. Front. Plant Sci. 8, 737. https://doi.org/10.3389/fpls.2017.00737.

Carrer, M., Unterholzner, L., Castagneri, D., 2018. Wood anatomical traits highlight complex temperature influence on Pinus cembra at high elevation in the eastern Alps. Int. J. Biometeorol. 62 (1745), 1753. https://doi.org/10.1007/s00484-018-1577-4.

Castagneri, D., Prendin, A.L., Peters, R., Carrer, M., von Arx, G., Fonti, P., 2020. Long-term impacts of defoliator outbreaks on larch xylem structure and wood biomass. Front. Plant Sci. 11, 1078. https://doi.org/10.3389/fpls.2020.01078.

Cerrato, R., Salvatore, M.C., Gunnarson, B.E., Linderholm, H.W., Carturan, L., Brunetti, M., De Blasi, F., Barono, C., 2019. A Pinus cembra L. tree-ring record for late spring to late summer temperature in the Rhaetian Alps, Italy. Dendrochronologia 53, 22–31. https://doi.org/10.1016/j.dendro.2018.10.010.

Cook, E.R., Kairiukstis, L.A., 1990. Methods of dendrochronology. Applications in the Environmental Sciences. International Institute for Applied Systems Analysis. Kluwer Academic Publishers, Dordrecht. https://doi.org/10.1007/978-94-015-7879-0 394 p.

Cook, E.R., Peters, K., 1981. The smoothing spline: a new approach to standardizing forest interior tree-ring width series for dendroclimatic studies. Tree-Ring Bull. 41, 45–53.

Cook, E.R., Briffa, K., Shiyatov, S., Mazepa, V., 1990. Tree-ring standardization and growth-trend estimation. In: Cook, E.R., Kairiukstis, L.A. (Eds.), Methods of Dendrochronology: Applications in the Environmental Sciences. Kluwer Academic Publisher, Dordrecht, The Netherlands, pp. 104–123.

Cook, E.R., Briffa, K.R., Meko, D.M., Graybill, D.A., Funkhouser, G., 1995. The 'segment length curse' in long tree-ring chronology development for palaeoclimatic studies. The Holocene 5, 229–237.

Cornes, R.C., Van Der Schrier, G., Van Den Besselaar, E.J.M., Jones, P.D., 2018. An ensemble version of the E-OBS temperature and precipitation data sets. J. Geophys. Res.-Atmos. 123 (17), 9391–9409. https://doi.org/10.1029/2017JD028200.

Corona, C., Guiot, J., Edouard, J.L., Chalié, F., Büntgen, U., Nola, P., Urbinati, C., 2010a. Millennium long summer temperature variations in the European Alps as reconstructed from tree rings. Clim. Past 6, 379–400. https://doi.org/10.5194/cp-6-379-2010.

Corona, C., Edouard, J.L., Guibal, F., Guiot, J., Bernard, S., Thomas, A., Denelle, N., 2010b. Long-term summer (751–2008) temperature fluctuation in the French Alps based on tree-ring data. Boreas 40, 351–366. https://doi.org/10.1111/j.1502-3885.2010.00185.x.

D'Arrigo, R., Wilson, R., Liepert, B., Cherubini, P., 2008. On the 'divergence problem' in northern forests: a review of the tree-ring evidence and possible causes. Glob. Planet. Chang. 60 (3), 289–305. https://doi.org/10.1016/j.gloplacha.2007.03.004.

Dauphin, B., Rellstab, C., Schmid, M., Zoller, S., Karger, D.N., Brodbeck, S., Guillaume, F., Gugerli, F., 2021. Genomic vulnerability to rapid climate warming in a tree species with a long generation time. Glob. Chang. Biol. 27, 1181–1195. https://doi.org/10.1111/gcb.15469.

Denne, M.P., 1988. Definition of latewood according to Mork (1928). IAWA J. 10, 59–62. https://doi.org/10.1163/22941932-90001112.

Dormont, L., Baltensweiler, W., Choquet, R., Roques, A., 2006. Larch-and pine-feeding host races of the larch bud moth (Zeiraphera diniana) have cyclic and synchronous population fluctuations. Oikos 115, 299–307. http://www.jstor.org/stable/40235280.

Edwards, J., Anchukaitis, K.J., Gunnarson, B.E., Pearson, C., Seftigen, K., von Arx, G., Linderholm, H.W., 2022. The origin of tree-ring reconstructed summer cooling in northern Europe during the 18th century eruption of Laki. Paleoceanogr. Paleoclimatol. 37, 2. https://doi.org/10.1029/2021PA004386.

Eilmann, B., Weber, P., Rigling, A., Eckstein, D., 2006. Growth reactions of Pinus sylvestris L. And Quercus pubescens willd. To drought years at a xeric site in Valais Switzerland. Dendrochronologia 23, 121–132. https://doi.org/10.1016/j. dendro.2005.10.002.

Esper, J., Cook, E.R., Krusic, P.J., Peters, K., Schweingruber, F.H., 2003. Tests of the RCS method for preserving low-frequency variability in long tree-ring chronologies. Tree-Ring Res. 59, 81–98. http://hdl.handle.net/10150/262573.

Esper, J., Frank, D.C., Wilson, R.J.S., Briffa, K.R., 2005. Effect of scaling and regression on reconstructed temperature amplitude for the past millennium. Geophys. Res. Lett. 32, L07711. https://doi.org/10.1029/2004GL021236.

Esper, J., Frank, D.C., Büntgen, U., Verstege, A., Luterbacher, J., Xoplaki, E., 2007. Long-term drought severity variations in Morocco. Geophys. Res. Lett. 34, L17702. https://doi.org/10.1029/2007GL030844.

EUFORGEN European forest genetic resources programme, 2014. Pinus cembra - EUFORGEN European forest genetic resources programme. Retrieved April 30, 2020, from http://www.euforgen.org/species/pinus-cembra/.

Fonti, P., García-González, I., 2004. Suitability of chestnut earlywood vessel chronologies for ecological studies. New Phytol. 163, 77–86. https://doi.org/10.1111/j.1469-8137.2004.01089.x.

Fonti, P., García-Gonzalez, I., 2008. Earlywood vessel size of oak as a potential proxy for spring precipitation in Mesic Sites. J. Biogeogr. 35, 2249–2257. https://doi.org/10.1111/j.1365-2699.2008.01961.x.

Fonti, P., von Arx, G., Garcia-Gonzalez, I., Eilmann, B., Sass-Klaassen, U., Gartner, H., Eckstein, D., 2010. Studying global change through investigation of the plastic responses of xylem anatomy in tree rings. New Phytol. 185, 42–53. https://doi.org/10.1111/j.1469-8137.2009. 03030.x.

Frank, D., Esper, J., 2005. Temperature reconstructions and comparisons with instrumental data from a tree-ring network for the European Alps. Int. J. Climatol. 25, 1437–1454. https://doi.org/10.1002/joc.1210.

Frank, D., Wilson, R., Esper, J., 2005. Synchronous variability changes in alpine temperature and tree-ring data over the past two centuries. Boreas 34, 498–505. https://doi.org/10.1080/03009480500231443.

Frank, D.C., Esper, J., Raible, C.C., Büntgen, U., Trouet, V., Stocker, B., Joos, F., 2010. Ensemble reconstruction constraints on the global carbon cycle sensitivity to climate. Nature 463 (7280), 527–U143. https://doi.org/10.1038/nature08769.

Fritts, H.C., 1976. Tree Rings and Climate. Academic Press, London.

Gagen, M., McCarroll, D., Loader, N.J., Robertson, I., Jalkanen, R., Anchukaitis, K.J., 2007. Exorcising the "segment length curse": summer temperature reconstruction since AD1640 using non-detrended stable carbon isotope ratios from pine trees in northern Finland. The Holocene 17, 433–444 10.1177%2F0959683607077012.

García-González, I., Souto-Herrero, M., Campelo, F., 2016. Ring-porosity and earlywood vessels: a review on extracting environmental information through time. IAWA J. 37 (2), 295–314. https://doi.org/10.1163/22941932-20160135.

Gärtner, H., Schweingruber, F.H., 2013. Microscopic Preparation Techniques for Plant Stem Analysis Kessel, Remagen.

Gleason, S.M., Ares, A., 2004. Photosynthesis, carbohydrate storage and survival of a native and an introduced tree species in relation to light and defoliation. Tree Physiol. 24 (10), 1087–1097. https://doi.org/10.1093/treephys/24.10.1087.

Gruber, A., Oberhuber, W., Gerhard, W., 2018. Nitrogen addition and understory removal but not soil warming increased radial growth of Pinus cembra at treeline in the central Austrian Alps. Front. Plant Sci. https://doi.org/10.3389/fpls.2018.00711.

Grudd, H., Briffa, K.R., Karlén, W., Bartholin, T.S., Jones, P.D., Kromer, B., 2002. A 7400-year tree-ring chronology in northern Swedish Lapland: natural climatic variability expressed on annual to millennial timescales. The Holocene 12, 657–665 10.1191%2F0959683602hl578rp.

Holmes, R.L., 1983. Computer-assisted quality control in tree-ring dating and measurement. Tree-Ring Bull. 43, 69–78.

Hughes, M.K., Swetnam, T.W., Diaz, H.F., 2011. Dendroclimatology: Progress and Prospects. Springer Science+Business Media B.V, Dordrecht.

IPCC, 2019. In: Pörtner, H.-O., Roberts, D.C., Masson-Delmotte, V., Zhai, P., Tignor, M., Poloczanska, E., Mintenbeck, K., Alegría, A., Nicolai, M., Okem, A., Petzold, J., Rama, B., Weyer, N.M. (Eds.), IPCC Special Report on the Ocean and Cryosphere in a Changing Climate. In press.

Jacoby, G.C., D'Arrigo, R., 1995. Tree-ring width and density evidence of climatic and potential forest change in Alaska. Glob. Biogeochem. Cycles 9, 227–234.

Jevšenak, J., Levanič, T., 2018. R package for studying linear and nonlinear responses between tree-rings and daily environmental data. Dendrochronologia 48, 32–39. https://doi.org/10.1016/j.dendro.2018.01.005.

Kulman, H.M., 1971. Effects of insect defoliation on growth and mortality of trees. Annu. Rev. Entomol. 16, 289–324.

Leal, S., Melvin, T.M., Grabner, M., Wimmer, R., Briffa, K.R., 2007. Tree ring-growth variability in the Austrian Alps: the influence of site, altitude, tree species and climate. Boreas 36, 426–440.

Leonelli, G., Pelfini, M., Battipaglia, G., Cherubini, P., 2009. Site- aspect influence on climate sensitivity over time of a high-altitude Pinus cembra tree-ring network. Clim. Chang. 96 (1), 185201. https://doi.org/10.1007/s10584-009-9574-6.

Lindholm, M., Eronen, M., 2000. A reconstruction of mid-summer temperatures from ring-widths of Scots pine since AD 50 in northern Fennoscandia. Geogr. Ann. 82 (4), 527–535. https://doi.org/10.1111/j.0435-3676.2000.00139.x.

Masson-Delmotte, V., Schulz, M., Abe-Ouchi, A., Beer, J., Ganopolski, A., Gonzalez Rouco, J.F., Jansen, E., Lambeck, K., Luterbacher, J., Naish, T., Osborn, T., Otto-Bliesner, B., Quinn, T., Ramesh, R., Rojas, M., Shao, X., Timmermann, A., 2013. Information from paleoclimate archives. In: Stocker, T.F., Qin, D., Plattner, G.-K., Tignor, M.M.B., Allen, S.K., Boschung, J., Nauels, A., Xia, Y., Bex, V., Midgley, P.M. (Eds.), Climate Change 2013: The Physical Science Basis: Contribution of Working Group I to the Fifth Assessment Report of the Intergovernmental Panel on Climate Change. Cambridge University Press, pp. 383–464 https://doi.org/10.1017/CBO9781107415324.013.

Melvin, M., Briffa, K.R., 2014. CRUST: software for the implementation of regional chronology standardisation: Part 1. Signal-free RCS. Dendrochronologia 32 (1), 7–20. https://doi.org/10.1016/j.dendro.2013.06.002.

Meteo Swiss, 2022. https://www.meteoswiss.admin.ch.

Myers, J.A., Kitajima, K., 2007. Carbohydrate storage enhances seedling shade and stress tolerance in a neotropical forest. J. Ecol. 95, 383–395. https://doi.org/10.1111/j.1365-2745.2006.01207.x.

Nola, P., Morales, M., Motta, R., Villalba, R., 2006. The role of larch budmoth (Zeiraphera diniana Gn.) on forest succession in a larch (Larix decidua Mill.) and Swiss stone pine (Pinus cembra L.) stand in the Susa Valley (Piedmont, Italy). Trees Struct. Funct. 20, 371–382. https://doi.org/10.1007/s00468-006-0050-x.

Oberhuber, W., 2004. Influence of climate on radial growth of Pinus cembra within the alpine timberline ecotone. Tree Physiol. 24, 291–301. https://doi.org/10.1093/treephys/24.3.291.

Oberhuber, W., Kofler, W., Pfeifer, K., Seeber, A., Gruber, A., Wieser, G., 2008. Long-term changes in tree-ring–climate relationships at Mt. Patscherkofel (Tyrol, Austria) since the mid-1980s. Trees 22 (1), 31–40. https://doi.org/10.1007/s00468-007- 0166-7.

Perkins-Kirkpatrick, S.E., Lewis, S.C., 2020. Increasing trends in regional heatwaves. Nat. Commun. 11, 3357. https://doi.org/10.1038/s41467-020-16970-7.

Prendin, A.L., Petit, G., Carrer, M., Fonti, P., Björklund, J., von Arx, G., 2017. New research perspectives from a novel approach to quantify tracheid wall thickness. Tree Physiol. 1–8. https://doi.org/10.1093/treephys/tpx037.

RStudio Team, 2020. RStudio: Integrated Development for R. RStudio, PBC, Boston, MA. http://www.rstudio.com.

Saulnier, M., Edouard, J.L., Corona, C., Guibal, F., 2011. Climate/growth relationships in a Pinus cembra high-elevation network in the Southern French Alps. Ann. For. Sci. 68, 189–200. https://doi.org/10.1007/s13595-011-0020-3.

Schär, C., Jendritzky, G., 2004. Hot news from summer 2003. Nature 432, 559–560. https://doi.org/10.1038/432559a.

Schweingruber, F.H., 1979. Auswirkungen des lärchenwickler- befalls auf die jahrring struktur der lärche. Schweiz. Z. Forstwes. 130, 1071–1093.

Schweingruber, F.H., 1985. Abrupt changes in growth reflected in tree ring sequences as an expression of biotic and abiotic influences. Inventorying and Monitoring Endangered Forests. Lufro Conference, Zurich, 291-295, Birmensdorf, Eidg. Anstaltfürdasforstliche versuchswesen.

Schweingruber, F.H., Johnson, S., 1993. Trees and Wood in Dendrochronology: Morphological, Anatomical, and Tree-ring Analytical Characteristics of Trees Frequently Used in Dendrochronology. Springer, New York.

Seftigen, K., Fonti, M.V., Luckman, B., Rydval, M., Stridbeck, P., von Arx, G., Wilson, R., Björklund, J., 2022. Prospects for dendroanatomy in paleoclimatology – a case study on Picea engelmannii from the Canadian Rockies. Clim. Pat. 18, 1151–1168. https://doi.org/10.5194/cp-18-1151-2022.

Știrbu, M.-I., Roibu, C.-C., Carrer, M., Mursa, A., Unterholzner, L., Prendin, A., 2022. Contrasting climate sensitivity of Pinus cembra tree-ring traits in the Carpathians. Front. Plant Sci. https://doi.org/10.3389/fpls.2022.855003.

Stokes, M.A., Smiley, T.L., 1968. Introduction to Tree-ring Dating. University of Chicago Press, Chicago.

Weidner, K., Heinrich, I., Helle, G., Löffler, J., Neuwirth, B., Schleser, G.H., Vos, H., 2010. Consequences of larch budmoth outbreaks on the climatic significance of ring width and stable isotopes of larch. Trees Struct. Funct. 24, pp. 399–409. https://doi.org/10.1007/s00468-010-0421-1.

Wigley, T.M., Briffa, K.R., Jones, P.D., 1984. On the average value of correlated time series, with applications in dendroclimatology and hydrometeorology. J. Clim. Appl. Meteorol. 23, 201–213.

Ziaco, E., Biondi, F., Heinrich, I., 2016. Wood cellular dendroclimatology: testing new proxies in Great Basin bristlecone pine. Front. Plant Sci. 7, 1602. https://doi.org/10.3389/fpls.2016.01602.